

Soft wall model for a holographic superconductor

S. S. Afonin and I. V. Pusenkov

V. A. Fock Department of Theoretical Physics, Saint-Petersburg State University, 1 ul. Ulyanovskaya, St. Petersburg, 198504, Russia
Email: afonin@hep.phys.spbu.ru, i.pusenkov@spbu.ru

Abstract

We apply the soft wall holographic model from hadron physics to a description of the high- T_c superconductivity. In comparison with the existing bottom-up holographic superconductors, the proposed approach is more phenomenological. On the other hand, it is much simpler and has more freedom for fitting the conductivity properties of the real high- T_c materials. We demonstrate some examples of emerging models and discuss a possible origin of the approach.

1 Introduction

Recently the holographic superconductors have attracted a lot of attention (see, e.g., reviews [1, 2]). They represent certain AdS/CFT models containing black holes and describe some important features of superconductivity. The active research in this direction was inspired by an observation made in Ref. [3] that such models could describe the high- T_c superconductivity discovered in some cuprates and other materials. This spectacular phenomenon in condensed matter has still not been understood [4]. It is not described by the standard BCS theory (a theory of weak inter-fermion interactions mediated by phonons) since it is caused by a strong coupling between fermions [5]. Due to the strong coupling the establishing of the ground state of the system becomes a hard problem. This state is not the Fermi liquid as in the BCS theory. One of possibilities for modelling the ground state in the high- T_c cuprates is the two-dimensional "tomographic Luttinger liquid" [6]. It is interesting that the expected ground state of the finite-density QCD (characterizing by the color superconductivity) might have a similar nature [7].

The practical applications of the gauge/gravity duality are not restricted by the strongly coupled gauge theories. The conformal behavior near the critical points of phase transitions suggested the idea to apply the methods of AdS/CFT correspondence to strongly coupled condensed matter systems [8]. In particular, this gave tantalizing prospects of finding a description for the high- T_c superconductivity in terms of a dual gravitational theory.

The simplest qualitative theory for holographic superconductor was constructed in Ref. [3]. It represents an Abelian–Higgs bottom-up holographic model with black hole. The model shares some similarities with the Ginzburg–Landau theory of superconductivity. All other bottom-up holographic superconductors proposed in the literature can be viewed as extensions of the model of Ref. [3]. The existing holographic models, both in the bottom-up and in the top-down approaches, give only a rough qualitative description of the real high- T_c materials. From the point of view of a condensed matter phenomenologist, it would be interesting to have a simple holographic superconductor with several adjustable parameters which would allow to fit the physical characteristics of a concrete superconducting material. In the present Letter, we propose a design for such a model.

The idea of our approach is borrowed from the soft wall (SW) holographic model in hadron physics [9]. The purpose of construction of the SW model was essentially the same — advancing in quantitative holographic description of real experimental data. The SW model is well tunable for description of the hadron spectra and related phenomenology, albeit it does not describe (at least in its simplest version) the spontaneous chiral symmetry breaking in QCD. Our SW holographic superconductors will be also quite flexible for fitting the observable properties of high- T_c superconductors, first of all the behavior of optical conductivity. However, we need to pay a similar price — the simplest SW superconductor does not describe the superconducting phase transition. Embedding this description seems to require a certain complication. But if we are interested in a description of experimentally measurable quantities, the approach that we propose should be considered as a step forward to building a phenomenologically useful holographic description of high- T_c superconductors. A pleasant feature of our approach is that the emerging models are much simpler than the original model of Ref. [3] which before has been regarded (in the probe limit) as the simplest holographic superconductor.

The structure of the paper is as follows. In order to make the text self-contained and to help in comparing our approach with the standard one, we remind the reader the idea of the first bottom-up holographic superconductor [3] in Section 2. Our SW superconductor is introduced in Section 3. Section 4 contains discussions and we conclude in Section 5. All plots are presented in Appendix.

2 The simplest standard model of a holographic superconductor

We will recall very briefly the basics of the first holographic model for the high- T_c superconductivity. This model was constructed as a 3+1 dimensional Einstein gravitational theory with a negative cosmological constant. By assumption, it is dual to a 2+1 dimensional superconductor. The dimensionality was dictated by the experimental fact that the high- T_c cuprates and other high- T_c materials are usually layered and much of the physics is effectively 2+1 dimensional. The model includes a $U(1)$ gauge field interacting (following an analogy with the Landau–Ginzburg theory of superconductivity) with a complex scalar field ψ . The action of the model is [3]

$$S = \int d^4x \sqrt{-g} \left(R + \frac{6}{L^2} - \frac{1}{4} F_{\mu\nu} F^{\mu\nu} - |\nabla\psi - iqA\psi|^2 - m^2\psi^2 \right), \quad (1)$$

where R is the scalar curvature, $F_{\mu\nu} = \nabla_\mu A_\nu - \nabla_\nu A_\mu$, L is the AdS radius. The most of the interesting physics appears already in the probe limit: $q \rightarrow \infty$ with qA_μ and $q\psi$ fixed. This limit simplifies considerably the model because the backreaction of the fields on the metric is neglected. As a background metric one considers the planar Schwarzschild AdS black hole

$$ds^2 = -f(r)dt^2 + \frac{dr^2}{f(r)} + r^2(dx^2 + dy^2), \quad (2)$$

$$f(r) = \frac{r^2}{L^2} \left(1 - \frac{r_0^3}{r^3} \right). \quad (3)$$

The Schwarzschild radius r_0 yields the Hawking temperature,

$$T = \frac{3r_0}{4\pi L^2}. \quad (4)$$

The black hole in this model is unstable and forms "scalar hair". To see this one looks for static translationally invariant solutions: $A_r = A_x = A_y = 0$, $A_t = \phi(r)$, $\psi = \psi(r)$. The equations of motion for ϕ and ψ with certain boundary conditions give the relevant solutions. In Ref. [3], the case $m^2 = -2/L^2$ was considered (we will set $L = 1$ in what follows). In this case, the solutions regular at the horizon have the following asymptotics at infinity,

$$\psi = \frac{\psi^{(1)}}{r} + \frac{\psi^{(2)}}{r^2} + \dots, \quad \phi = \mu - \frac{\rho}{r} + \dots, \quad (5)$$

where μ and ρ are interpreted as the chemical potential and charge density of the dual field theory. If we set $\psi^{(1)} = 0$, the behavior of the condensate

$\langle O_2 \rangle = \psi^{(2)}$ as a function of temperature is depicted in Fig. 1 (see Appendix). As $T \rightarrow T_c$, the behavior is $\langle O_2 \rangle \sim (1 - T/T_c)^{1/2}$ as in the Landau–Ginzburg theory [3].

The plot in Fig. 1 is obtained in the following way. By symmetry, $\psi^{(2)}$ is a function of $r_0/\sqrt{\rho}$. One solves numerically the system of equations of motion at fixed ρ and, using (4), the critical temperature T_c is defined as $\psi^{(2)}(T_c/\sqrt{\rho}) = 0$. Thus, $T_c \sim \sqrt{\rho}$ and one can draw the plot in Fig. 1 in units of T_c .

An important measurable quantity in superconductors is the optical conductivity (the conductivity as a function of frequency). By symmetry, it is enough to analyze the conductivity in the x direction. Consider the perturbations of the vector field in the form

$$A_\mu = A_x(r)e^{i\omega t}. \quad (6)$$

The linearized equation of motion reads

$$A_x'' + \frac{f'}{f} A_x' + \left(\frac{\omega^2}{f^2} - \frac{2\psi^2}{f} \right) A_x = 0. \quad (7)$$

The causal behavior is provided by the ingoing wave boundary condition at the horizon [3],

$$A_x \sim f^{-i\omega/3r_0}. \quad (8)$$

The asymptotic behavior at infinity is

$$A_x = A_x^{(0)} + \frac{A_x^{(1)}}{r} + \dots \quad (9)$$

Since the behavior (9) holds near the AdS boundary the gauge/gravity correspondence [10] tells us that $A_x^{(0)}$ must be identified with the source and $A_x^{(1)}$ is dual to the induced current J_x . Then the definition of the conductivity and the ansatz (6) result in

$$\sigma(\omega) = \frac{J_x}{E_x} = \frac{J_x}{-\dot{A}_x^{(0)}} = \frac{-iA_x^{(1)}}{\omega A_x^{(0)}}. \quad (10)$$

The typical behavior of real and imaginary parts of $\sigma(\omega)$ at $m^2 = -2$ is shown in Figs. 2 and 3. This behavior looks similar to the experimental data on the AC conductivity for the high- T_c superconductors reproduced¹ in Figs. 4 and 5. The optical conductivity is constant above T_c , below T_c it develops

¹The gate voltage in those figures plays the role of the current density which fixes the temperature scale in the model.

a gap at some frequency ω_g which can be identified with the minimum of $\text{Im}[\sigma(\omega)]$ [11]. The gap is the most pronounced in the limit $T \rightarrow 0$. In this limit $\sqrt{\langle O_2 \rangle}/T_c \simeq 7$ (see Fig. 1). In the same limit one can calculate $\omega_g/\sqrt{\langle O_2 \rangle} \simeq 1.2$. Both relations turn out to be weakly dependent on the choice of parameters. Excluding $\sqrt{\langle O_2 \rangle}$, one arrives at an approximately (within 10%) universal relation

$$\frac{\omega_g}{T_c} \simeq 8.4. \quad (11)$$

The obtained relation (11) is quite remarkable. First, it is close to that in the high- T_c superconductors [12]. Second, the comparison with the BCS value $\omega_g \simeq 3.5T_c$ shows that the holographic model under consideration seems to describe a system at strong coupling.

At this point we should make a remark that will be crucial for constructing our model in the next Section. The black hole (2) is invariant under the rescaling

$$r \rightarrow \lambda r, \quad (t, x, y) \rightarrow (t, x, y)/\lambda, \quad r_0 \rightarrow \lambda r_0. \quad (12)$$

This entails the invariance $\omega \rightarrow \lambda\omega$ and (by (4)) $T \rightarrow \lambda T$ leading to the scale invariance of the ratio ω/T . The positions of minima $\left(\frac{\omega}{\lambda T_c}\right)_{\min}$ in Fig. 3 can be viewed as $\frac{1}{\lambda} \frac{\omega_g}{T_c}$. Thus, the ratio (11) can be obtained from any plot in Fig. 3 just multiplying by λ the position of the corresponding minimum.

The observation above hints at the possibility to construct the holographic superconductors without condensates. Such models should respect the scaling symmetry (12) and reproduce the experimental plots in Figs. 4 and 5 as close as possible. After that one can simply extract the ratio (11). Below we build some examples for such models.

3 Soft wall holographic superconductor

There exist common features in constructing the bottom-up holographic models for superconductivity and for hadron physics. The solution of equations of motion should yield the optical conductivity in the former case and the correlation functions (with ensuing hadron spectrum) in the latter one. The first bottom-up model for hadrons was proposed in Ref. [13]. The action of this model looks like a five-dimensional extension of (1). The condensation of the scalar field ψ described the spontaneous chiral symmetry breaking in QCD. An axial-vector field was also introduced in order to get the chiral dynamics and the mass splitting between the vector and axial mesons. Thus one deals with very similar equations but imposes completely different

requirements on the solutions. The important differences in the bottom-up description of hadrons in Ref. [13] are as follows: a) In the probe limit, the background metric is pure AdS (unless one is interesting in some finite-temperature effects); b) The infrared cutoff r_{IR} is introduced by hands to provide the mass scale (for this reason the model of Ref. [13] is referred to as the "hard wall" model); c) The scalar field ψ condenses first, i.e. the vector fields do not enter the equation of motion for ψ .

The hard wall model describes well the chiral dynamics but gives very rough predictions for the hadron spectrum. In order to improve the second aspect the so-called "soft wall" holographic model was introduced in Ref. [9]. The action of the simplest SW model describing the vector spectrum is

$$S_{\text{SW}} = \int d^5x \sqrt{|g|} e^{-2\varphi(ar)} \left(-\frac{1}{4} F_{MN} F^{MN} \right). \quad (13)$$

Now there is no infrared cutoff and the mass scale is provided by the parameter a . The experimental (or theoretically expected) spectrum can be fine-tuned by a choice of the dilaton background φ . Simultaneously, one may reproduce much better the structure of the Operator Product Expansion of the QCD correlation functions. In principle, the dilaton background may be formally (i.e. neglecting a surface term) eliminated by the substitution $A_M \rightarrow e^\varphi \tilde{A}_M$. The price to pay is the appearance of r -dependent mass term for \tilde{A}_M . However, the model can be reformulated in a gauge-invariant way if we assume that this term emerges from condensation of some scalar field ψ [14]. In particular, the standard choice $\varphi \sim r^{-2}$ [9] leads to the (five-dimensional extension of) field part of action (1) with $m^2 = -4$ [14]. In such a "no-wall" model it is assumed that the field ψ condenses first and only after that one analyses the ensuing phenomenology.

We are going to use the analogy from the hadron physics as the starting point for construction of the SW holographic superconductor. Consider the action

$$S = \int d^4x \sqrt{-g} e^{-2h\left(\frac{r}{r_0}\right)} \left(-\frac{1}{4} F_{\mu\nu} F^{\mu\nu} \right). \quad (14)$$

The background metric is the black hole one (2). By assumption, the dilaton profile $-2h\left(\frac{r}{r_0}\right)$ emerges due to condensation of some scalar field and satisfies the scaling invariance (12). Making use of the ansatz (6) in the equation of motion, we arrive at the equation

$$A_x'' + \left(\frac{f'}{f} - 2h' \right) A_x' + \frac{\omega^2}{f^2} A_x = 0. \quad (15)$$

As in the "no-wall" model for hadrons, one can eliminate the dilaton background in (14) by the substitution $A_x \rightarrow e^h A_x$ and come to the action

$$S = \int d^4x \sqrt{-g} \left\{ -\frac{1}{4} F_{\mu\nu} F^{\mu\nu} + \frac{f}{2} \left[h'' - (h')^2 + h' \frac{f'}{f} \delta_{ki} + \frac{2h'}{r} \delta_{0i} \right] A_i A^i \right\}. \quad (16)$$

Here $i = 0, 1, 2$; $k = 1, 2$. We can choose the gauge $A_r = 0$ where the second term is proportional to $A_\mu A^\mu$, i.e. it becomes the genuine mass term. The theories (14) and (16) are equivalent if the following surface terms are absent,

$$\int d^3x \sqrt{-g} h' A_0^2 \Big|_{r=r_0}^{r=\infty} = 0, \quad (17)$$

$$\int d^3x h' f A_k^2 \Big|_{r=r_0}^{r=\infty} = 0. \quad (18)$$

Now we can rewrite (16) in the form of (1) with some potential $V(\psi)$ instead of the mass term $m^2 \psi^2$. The solution of equation of motion for ψ in the absence of A_μ must reproduce the mass term in (16), this dictates the form of the potential $V(\psi)$.

The action (16) leads to the equation of motion

$$A_x'' + \frac{f'}{f} A_x' + \left[\frac{\omega^2}{f^2} + h'' - (h')^2 + h' \frac{f'}{f} \right] A_x = 0. \quad (19)$$

It is easy to check that the substitution $A_x \rightarrow e^h A_x$ converts Eq. (15) to Eq. (19). The latter has the form of Eq. (7). The term containing ψ in Eq. (7), which was a numerical solution of coupled system of equations in Ref. [3], is replaced in Eq. (19) by a term completely dictated by the function h . We are free to choose this function phenomenologically.

Consider the possibilities $h = r_0/r$ and $h = (r_0/r)^2$, where the scaling (12) is taken into account. They correspond to solutions with condensates $\langle O_1 \rangle$ and $\langle O_2 \rangle$ in (5). The resulting behavior of optical conductivities $\sigma(\omega)$ is displayed in Figs. 6 and 7, respectively. The obtained shapes recover (at least qualitatively) the results of Ref. [3]. These two differing shapes are expected for superconductors having the so-called type II and type I coherence factors.

The considered possibilities can be generalized to the ansatz

$$h = \alpha \left(\frac{r_0}{r} \right)^\beta. \quad (20)$$

We may vary the parameter α at fixed β and vice versa and look at the behavior of optical conductivity. A couple of corresponding examples are

demonstrated in Figs. 8, 9 and 10, 11, respectively. A non-polynomial ansatz for h can be chosen. An example is presented in Figs. 12 and 13.

The plots in Figs. 6-13 seem to share the following common property: At any reasonable ansatz for h , when the form of curves become maximally close to the experimental ones in Figs. 4 and 5, the minimal value of $\text{Im}[\sigma(\omega)]$ lies in the vicinity of the region $\omega/r_0 \simeq 2$. According to our discussions at the end of Section 2 and to relation (4) for $L = 1$, $r_0 \approx 4.2T$, we have $\frac{\omega_g}{4.2T_c} \simeq 2$, i.e. we obtain a rough estimate for the gap coinciding² with (11).

This agreement looks surprising. It means that if a holographic superconductor (in the probe limit) reproduces well the behavior of the optical conductivity then the gap is approximately universal (more strictly, of the same order of magnitude) for such models due to the scaling symmetry. Even more surprising is that the value of this gap is often close to that in the high- T_c cuprates [12].

The plots of $\text{Re}[\sigma(\omega)]$ in Fig. 8 shows a formation of gap with changing α . This suggests that in reality α should be a decreasing function of T , say a positive power of $(1 - T/T_c)$. The parameter β may also include a temperature dependence with some critical value, moreover, it might be responsible for the coherence factor type.

The main lesson of the exercises above is that given a concrete superconducting material, in principle, one is able to find phenomenologically the form of the dilaton background h that interpolates the observable superconducting properties of this material. Then one can use the obtained h to interpolate the properties of other known high- T_c superconductors and reveal the required change of input parameters. This would help to ascribe a physical meaning to the model parameters. Next step would be a derivation of a phenomenologically reasonable form(s) of h from a consistent gauge/gravity theory. As usual, this step is the most difficult.

In the probe limit, the form of the dilaton profile $-2h\left(\frac{r}{r_0}\right)$ should follow from an action

$$S_\varphi = \int d^4x \sqrt{-g} \left(-\frac{1}{2} \partial_\mu \varphi \partial^\mu \varphi - V(\varphi) \right), \quad (21)$$

with the black hole metric (2). A solution of equation of motion should yield $\langle \varphi \rangle \equiv h$. The potential $V(\varphi)$ can be restored from the form of $h\left(\frac{r}{r_0}\right)$. For

²We have tried many probe functions for h . A more accurate estimate is $\omega/r_0 \simeq 1 - 3$ leading to the gap in the range $\omega_g/T_c \simeq 4 - 12$.

instance, if we choose $2h = \left(\frac{r}{r_0}\right)^\beta$ then

$$V = \beta \left[\frac{1}{2}(\beta + 3)\varphi^2 - \frac{\beta^2 r_0^3}{2 - 3/\beta} \varphi^{2-3/\beta} \right]. \quad (22)$$

Imposing the Breitenlohner–Freedman boundary for the scalar mass in the AdS_{d+1} space-time [15], $m^2 \geq -\frac{d^2}{4L^2}$, we have $\beta(\beta + 3) \geq -9/4$ that leads to $(\beta - 3/2)^2 \geq 0$, i.e. any value of β is allowed, with the value $\beta = -3/2$ providing the minimal mass. The second term in (22) looks unnatural since it emerges due to the horizon and contains a non-integer power of interaction except some special cases. This situation is quite general. If we take the point of view that in the holographic approach, which is inherently large- N one, only quadratic in fields part is relevant, then we should either assume $r_0 = 0$ in (22), i.e. somehow motivate pure AdS metric in (21), or exclude the interaction term. In the latter case, the equation of motion for $\varphi = \varphi(r)$,

$$-(r(r^3 - r_0^3)\varphi')' + r^2\beta(\beta + 3)\varphi = 0, \quad (23)$$

has solutions in terms of the Legendre functions of the first (P) and second (Q) kind,

$$\varphi^{(1)} = P_{\beta/3} \left(1 - \frac{2r^3}{r_0^3} \right), \quad \varphi^{(2)} = Q_{\beta/3} \left(1 - \frac{2r^3}{r_0^3} \right). \quad (24)$$

The energy functional of the action (21) is minimal at $\beta = -3/2$. Accepting this value and choosing³ $h = Q_{-1/2}(1 - 2(r/r_0)^3)$ in (14), we obtain a realistic prediction for the optical conductivity which is depicted as one of plots in Figs. 14 and 15.

For comparison, we reproduce in Fig. 16 a certain experimental plot for $\text{Re}[\sigma(\omega)]$ demonstrating the difference of the shape below and above the critical temperature T_c . It is seen that in reality the parameter β in (22) should depend on T achieving a critical value between $\beta/3 = -0.7$ and $\beta/3 = -0.75$ where the local minimum in $\text{Re}[\sigma]$ disappears. In contrast to the Landau–Ginzburg theory, the quadratic part of the potential (22) does not vanish at the critical point. This feature could have a natural interpretation — the high- T_c superconductors represent doped materials and their T_c depends crucially on the density of doped holes x that lies in a finite interval $a < x < b$ [4]. The maximal T_c roughly corresponds to $x = (a + b)/2$ (the optimal doping). Thus the parameter β in (22) might encode a dependence on the doping x .

³The choice $h = P_{-1/2}(1 - 2(r/r_0)^3)$ does not satisfy the boundary condition (8).

4 Discussions

The presented approach to building a bottom-up holographic superconductor is more phenomenological than the original one [3]. It would be interesting to clarify a possible origin of our approach. The SW holographic model in hadron physics cannot help because its relation to any fundamental string theory is unknown. The full action for the considered holographic superconductor is

$$S = \kappa_1 S_{\text{grav}} + \kappa_2 S_\varphi + \kappa_3 S_{\varphi,A}. \quad (25)$$

Our approach is justified if

$$\kappa_1 \gg \kappa_2 \gg \kappa_3. \quad (26)$$

By assumption, the part $\kappa_1 S_{\text{grav}}$ gives the black hole metric (2) and the back-reaction to the metric from $\kappa_2 S_\varphi$ and $\kappa_3 S_{\varphi,A}$ can be neglected due to (26). After that we find $\langle\varphi\rangle$ from minimum of S_φ and then extract the phenomenology from $S_{\varphi,A}$. Following the analogy with the SW model in hadron physics [9], we have chosen the interaction of the scalar field φ with the gauge field A in the form $e^\varphi F_{\mu\nu}^2$. In principle, such coupling is provided by some known dilatonic black holes unstable to forming the scalar hair [1]. However, this possibility has not been exploited in holographic superconductors because $F_{\mu\nu}^2$ acts as a source for φ , so $\langle\varphi\rangle \neq 0$ for any charged black hole [1]. In our case, the given argument does not apply since, first, φ in the exponent represents a fixed background, second, we are free to choose a different coupling, say, $e^{\varphi^2} F_{\mu\nu}^2$.

How the action (25) with the sequence of scales (26) may follow from a string theory is an open problem. In the case of holographic dual for a conformal $SU(N)$ gauge theory, one has $\kappa_1 = \mathcal{O}(N^2)$. We may implement (26) assuming the scaling

$$\kappa_1 = \mathcal{O}(N^2), \quad \kappa_2 = \mathcal{O}(N), \quad \kappa_3 = \mathcal{O}(1), \quad (27)$$

at large N . This scaling entails the question about the physical meaning of N in the holographic superconductors. The given question is tightly related with a long standing problem concerning the analog of large- N limit in condensed matter systems [1].

Perhaps the answer lies in the structure of high- T_c superconductors. They represent small pieces of layered materials [12]. Imagine that N is the number of layers. Imagine further that each layer interacts with all (or a substantial part of) other layers. Then we have $\mathcal{O}(N^2)$ interactions and the corresponding background medium is described in the action (25) by the part $\kappa_1 S_{\text{grav}}$ with $\kappa_1 = \mathcal{O}(N^2)$. Since in the experimental patterns the layers are weakly

coupled [1], we should have a weakly coupled gravitational theory as it is required by the AdS/CFT correspondence. Assume that the medium inside each layer can be modelled by a relativistic theory of the scalar field φ . Since we have N layers, in (25) the contribution S_φ emerges with $\kappa_2 = \mathcal{O}(N)$. The real high- T_c materials can have several sorts of layers composed of different atoms. So, strictly speaking, we should consider several fields φ_i . But we simplify the situation. The part $\kappa_3 S_{\varphi,A}$ describes a response of the system to the electromagnetic field. This response is unrelated to the number of layers, thus $\kappa_3 = \mathcal{O}(1)$.

The outlined physical picture could justify the choice of the action (25) with the behavior of constants (27) at large N . In some sense, within this interpretation a layered material resembles the stack of N branes in the AdS/CFT correspondence [16]. Such a resemblance might be among reasons why the gauge/string duality can be successfully applied to the high- T_c superconductors.

In our approach, the dilaton profile comes from condensation of a scalar field. This description should be dual to a theory of S-wave superconductors. Many real high- T_c superconductors are known to have the D -wave (the cuprates) or sometimes P -wave superconductivity [12]. The construction of the corresponding extensions is straightforward — one should replace the contribution S_φ in (25) by an action for the vector or tensor field that condenses and forms the dilaton profile in $S_{\varphi,A}$. In principle, the vector or tensor condensate can be made anisotropic and, hence, describe the anisotropic (striped) superconductivity.

5 Conclusions

A fruitful interrelation between particle physics and superconductivity in condensed matter started in early 60-th when Nambu and Jona-Lasinio proposed their famous model for the nucleons from an analogy with the theory of superconductivity [17]. Recently the story has taken an interesting turn with the appearance of the holographic approach inspired by the gauge/gravity duality in string theory. It turned out that the concept of the bottom-up holographic models originally developed for the hadron physics can be applied to the high- T_c superconductors [3], the nature of which remains enigmatic. Unfortunately the existing holographic superconductors are still very far from any quantitative description of the real high- T_c materials. In this respect, the progress in the holographic hadron physics is more considerable.

In the present work, we have made an attempt to advance in the quantitative holographic description of the high- T_c superconductors. For this purpose

we applied the idea of the soft wall holographic model from hadron physics [9]. The phenomenological description of the form of the optical conductivity in our approach is in one-to-one correspondence with the phenomenological description of the form of the hadron spectrum in the standard SW model [9]. The simplest model of holographic superconductor is believed to be the one proposed in the original paper [3]. We have shown that it is possible to construct much simpler models. The simplicity is likely the main advantage of the proposed SW holographic superconductors. In hadron physics, the SW model does not describe (without significant complications) the dynamics of the chiral symmetry breaking but in description of the observable spectrum it seems to be the most successful bottom-up holographic approach. In the holographic superconductors, we have a similar situation: The considered SW model (in its current form) does not describe the phase transition to superconductivity, but if we are interested in the experimentally measurable quantities like optical conductivity, the SW superconductors are able to describe the emerging phenomenology more realistically than many other holographic superconductors.

There are various directions for extensions and applications of the proposed approach. We mention some of them. (i) It would be interesting to identify the most reasonable dilaton profiles from the best fit to the experimental data on the optical conductivities. (ii) One can calculate other transport properties and study the response to the non-zero chemical potential and magnetic field. (iii) At some choices of the dilaton profile the SW model seems to describe a superinsulator and this could be interesting. (iv) Perhaps the phase transition to superconductivity can be modelled as the Hawking-Page phase transition in the gravitational part of (25) from the thermal AdS space to AdS with black hole [18]. The transition point could relate the critical temperature to some dimensional model parameter (as in Ref. [19] for the deconfinement temperature). The requirement to describe the transport properties of the high- T_c materials above T_c may then restrict significantly a possible form of the dilaton profile. (v) Among theoretical challenges for the holographic superconductors one can mention the problem of a dual gravitational interpretation for the empirical Homes' scaling law in the high- T_c superconductors [20]. Our preliminary analysis showed that this law imposes rather strong constraint on the mutual dependence of the model parameters and seems to prescribe for them a certain temperature dependence. We hope to address at least some of the issues above in the future work.

Acknowledgments

The authors acknowledge Saint-Petersburg State University for research grants 11.38.189.2014 and 11.38.660.2013. The work was also partially supported by the RFBR grant 13-02-00127-a.

References

- [1] G. T. Horowitz, Lect. Notes Phys. **828**, 313 (2011).
- [2] R. G. Cai, L. Li, L. F. Li and R. Q. Yang, Sci. China Phys. Mech. Astron. **58**, 060401 (2015).
- [3] S. A. Hartnoll, C. P. Herzog and G. T. Horowitz, Phys. Rev. Lett. **101**, 031601 (2008).
- [4] E. W. Carlson, V. J. Emery, S. A. Kivelson and D. Orgad, arXiv:cond-mat/0206217.
- [5] A. J. Leggett, Nature Physics, **2** 134 (2006).
- [6] P. W. Anderson, " *The Theory of Superconductivity in the High- T_c Cuprates*", Princeton University Press, Princeton, 1997.
- [7] E. Shuster and D. T. Son, Nucl. Phys. B **573**, 434 (2000).
- [8] S. A. Hartnoll, Class. Quant. Grav. **26**, 224002 (2009).
- [9] A. Karch, E. Katz, D. T. Son and M. A. Stephanov, Phys. Rev. D **74**, 015005 (2006).
- [10] E. Witten, Adv. Theor. Math. Phys. **2**, 253 (1998); S. S. Gubser, I. R. Klebanov and A. M. Polyakov, Phys. Lett. B **428**, 105 (1998).
- [11] G. T. Horowitz and M. M. Roberts, Phys. Rev. D **78**, 126008 (2008).
- [12] K. K. Gomes *et al.*, Nature **447**, 569 (2007).
- [13] J. Erlich, E. Katz, D. T. Son and M. A. Stephanov, Phys. Rev. Lett. **95**, 261602 (2005); L. Da Rold and A. Pomarol, Nucl. Phys. B **721**, 79 (2005).
- [14] S. S. Afonin, Int. J. Mod. Phys. A **26**, 3615 (2011).
- [15] P. Breitenlohner and D. Z. Freedman, Annals Phys. **144**, 249 (1982).

- [16] O. Aharony *et al.*, Phys. Rept. **323**, 183 (2000).
- [17] Y. Nambu and G. Jona-Lasinio, Phys. Rev. **122**, 345 (1961).
- [18] S. W. Hawking and D. N. Page, Commun. Math. Phys. **87**, 577 (1983).
- [19] C. P. Herzog, Phys. Rev. Lett. **98**, 091601 (2007).
- [20] C. C. Homes *et al.*, Nature **430**, 539 (2004).
- [21] Z. Q. Li *et al.*, Nature Physics **4**, 532 (2008).
- [22] D. van der Marel *et al.*, Nature **425**, 271 (2003).

Appendix: Plots

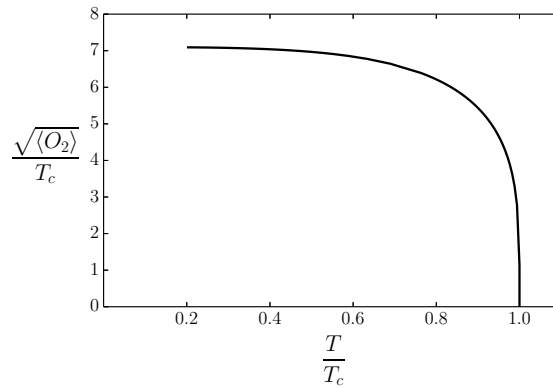


Fig. 1. The condensate $\langle O_2 \rangle$ as a function of temperature for $m^2 = -2$ [2].

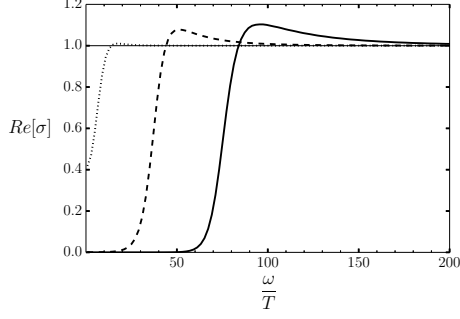


Fig. 2. The real part of the optical conductivity as a function of frequency normalized by temperature for $m^2 = -2$. Curves from left to right correspond to $\frac{T}{T_c} = \lambda \approx 0.888$ (dotted), $\lambda \approx 0.222$ (dashed) and $\lambda \approx 0.105$ (solid) [2].

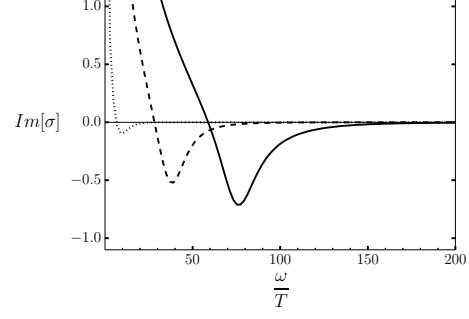


Fig. 3. The imaginary part of the optical conductivity from Fig. 2 [2].

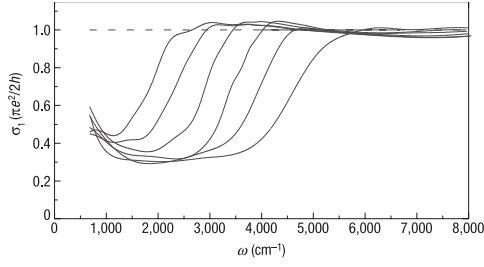


Fig. 4. The optical conductivity measured in graphene [21]. The curves from left to right correspond to the gate voltage 0, 10, 17, 28, 40, 54, 71 V.

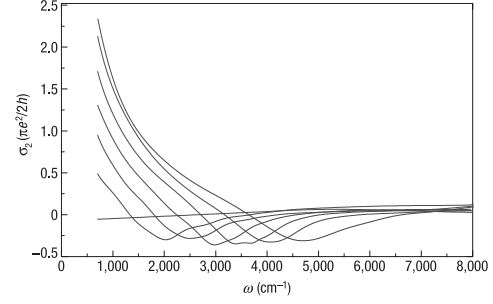


Fig. 5. The imaginary part of the conductivity from Fig. 4 [21].

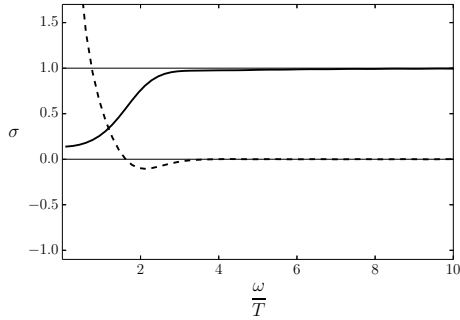


Fig. 6. The optical conductivity at $h = r_0/r$. The solid line corresponds to $\text{Re}[\sigma]$ and the dashed one to $\text{Im}[\sigma]$.

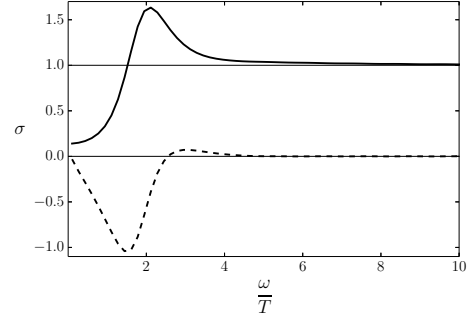


Fig. 7. The optical conductivity at $h = (r_0/r)^2$. The notations are as in Fig. 6.

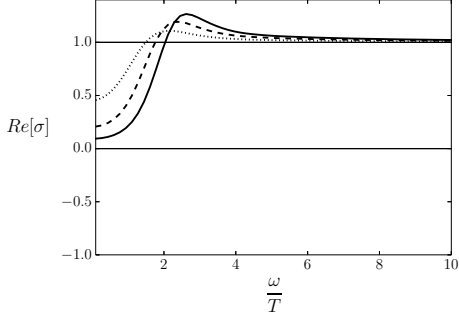


Fig. 8. $\text{Re}[\sigma]$ at $h = \alpha \left(\frac{r_0}{r}\right)^{1.4}$. From left to right $\alpha = 0.4$ (dotted), $\alpha = 0.8$ (dashed) and $\alpha = 1.2$ (solid).

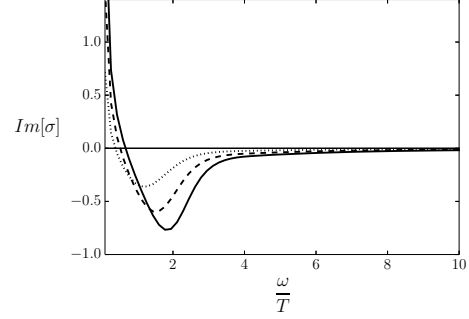


Fig. 9. $\text{Im}[\sigma]$ corresponding to the plots in Fig. 8.

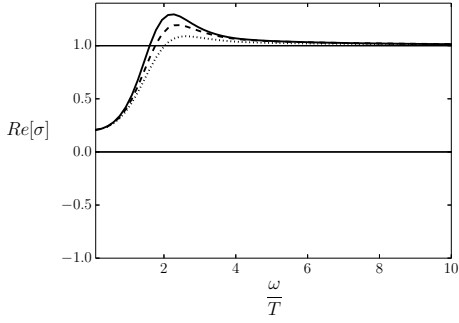


Fig. 10. $\text{Re}[\sigma]$ at $h = 0.8 \left(\frac{r_0}{r}\right)^\beta$. From right to left $\beta = 1.2$ (dotted), $\beta = 1.4$ (dashed) and $\beta = 1.6$ (solid).

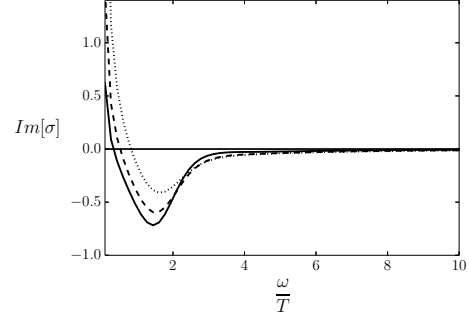


Fig. 11. $\text{Im}[\sigma]$ corresponding to the plots in Fig. 10.

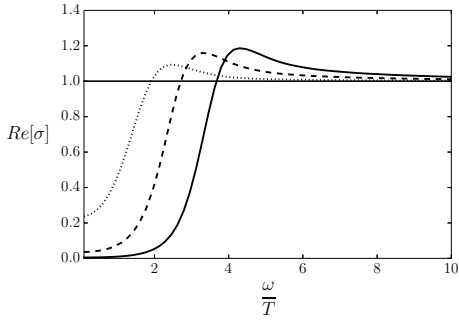


Fig. 12. $\text{Re}[\sigma]$ at $h = \log \left(\cosh \left(\frac{1}{2} + \alpha \frac{r_0}{r} \right) \right)$. From left to right we take $\alpha = 1$ (dotted), $\alpha = 2$ (dashed) and $\alpha = 3$ (solid).

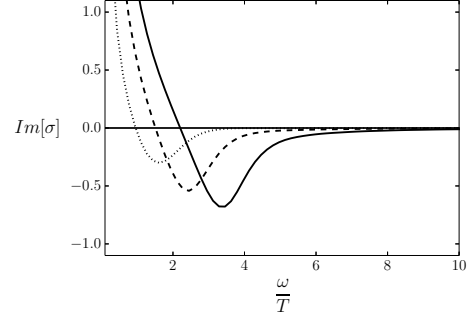


Fig. 13. $\text{Im}[\sigma]$ corresponding to the plots in Fig. 12.

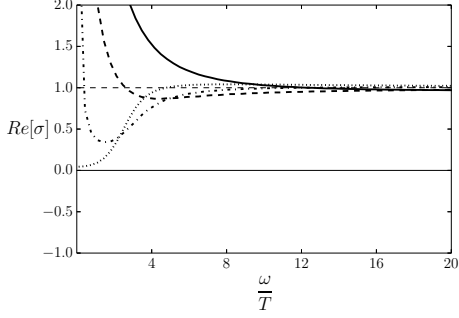


Fig. 14. $\text{Re}[\sigma]$ at $h = Q_\nu(1 - 2(r/r_0)^3)$. From left to right $\nu = -0.5$ (with an approximate δ -function at $\frac{\omega}{T} = 0$), $\nu = -0.6$, $\nu = -0.7$, $\nu = -0.75$.

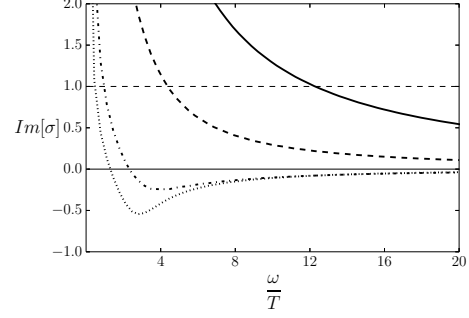


Fig. 15. $\text{Im}[\sigma]$ corresponding to the plots in Fig. 14.

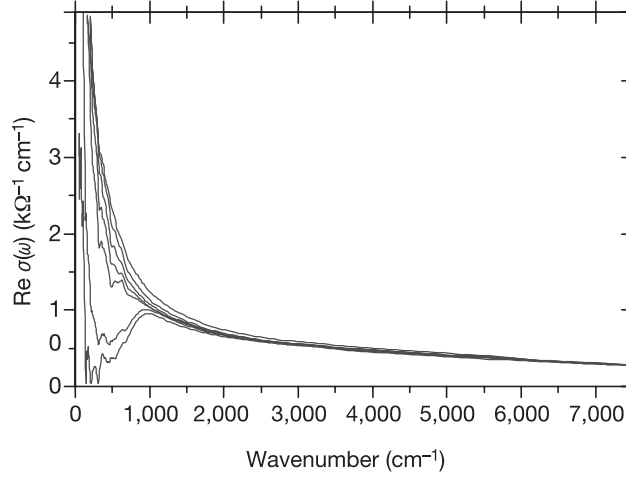


Fig. 16. The real part of the optical conductivity along the copper-oxygen planes of $\text{Bi}_2\text{Sr}_2\text{Ca}_{0.92}\text{Y}_{0.08}\text{Cu}_2\text{O}_{8+\delta}$ for a selected number of temperatures. Temperatures from left to right are 7, 50, 95, 130, 160, 200, 260 K. The critical temperature is 96 K. Experimental plot from Ref. [22].